Eur Biophys J (2000) 29: 542–548
DOI 10.1007/s002490000092

BIOPHYSICS LETTER

Reinhard Lipowsky · Thomas Harms

Molecular motors and nonuniform ratchets

Received: 27 April 2000 / Accepted: 9 May 2000 / Published online: 2 September 2000

Abstract Dimeric kinesin presumably moves in a "hand-over-hand" fashion via alternating steps of its two heads, which can cooperate in various ways. This motion is discussed in the framework of nonuniform ratchet models in which the molecular motor is described by M internal states and undergoes transitions at K spatial locations within the period of the molecular force potentials. Two subclasses of models with $(M, K) = (3, 2)$ and $(M, K) = (2, 2)$ are studied which correspond to weakly and strongly cooperative heads, respectively. Both subclasses lead to the same universal relationship between the motor velocity and the unbinding rate constant of the motor heads which is reminiscent of, but distinct from, Michaelis-Menten kinetics.

Key words Molecular motors · Kinesin · Ratchets · Michaelis-Menten kinetics · Force dependence

Introduction

Biological cells and subcellular organelles undergo directed motion during many essential biological processes such as cell locomotion, intracellular transport, or cell division. This motion is powered by molecular motors which are able to provide a direct coupling between chemistry and mechanics, i.e., to transduce the free energy released from chemical reactions directly into mechanical work.

One specific motor which has been experimentally studied in much detail is dimeric kinesin, which moves on microtubules (Howard et al. 1989; Svoboda et al. 1993; Hua et al. 1997; Schnitzer and Block 1997; Gilbert et al. 1998; Hancock and Howard 1998; Thormählen et al. 1998; Visscher et al. 1999). The microtubule is a linear filament consisting of 13 protofilaments of tubulin molecules which form a hollow cylinder. Each protofilament represents a one-dimensional lattice with a lattice constant of 8 nm. The motor consists of two identical amino acid chains which form two heads. Each kinesin head can act as an ATPase which adsorbs and hydrolyses ATP. In addition, each head can bind to and unbind from the microtubule. Thus, each head has an ATP-adsorption domain and a microtubule-binding domain.

Dimeric kinesin requires both heads in order to make many successive steps (e.g., see Hancock and Howard 1998). Each step corresponds to a center-of-mass movement of 8 nm (Svoboda et al. 1993; Hua et al. 1997; Schnitzer and Block 1997). In its rigor state, the two heads are bound to two successive lattice sites separated by 8 nm (Thormählen et al. 1998). All of these features are consistent with the intuitive picture that the motor advances via alternating 16 nm steps by each of its heads in a "hand-over-hand" fashion.

It is, however, still difficult to construct a unique model for this "hand-over-hand" motion since the two heads and their enzymatic cycles may cooperate in various ways (Gilbert et al. 1998; Hancock and Howard 1998). Thus, we will study two different classes of molecular motor models, which correspond to weakly and strongly cooperative heads, respectively, and will emphasize those features which are valid in both types of models. One such feature is the relationship between the motor velocity and the unbinding rate constant of the motor heads.

The unbinding rate constant may be expressed in terms of the ATP concentration. In this way, our models also lead to Michaelis-Menten-type relationships between the motor velocity and the ATP concentration which provide a good fit to the experimental data (Howard et al. 1989; Hua et al. 1997; Schnitzer and Block 1998; Visscher et al. 1999). In contrast, the dependence of the velocity on the applied force F is nonuniversal and depends on the underlying molecular interaction potentials.

R. Lipowsky (✉) · T. Harms
MPI für Kolloid- und Grenzflächenforschung,
Am Mühlenberg, 14476 Golm,
Germany
E-mail: lipowsky@mpikg-golm.mpg.de

In this article, we use the theoretical framework of composite Markov processes (or reaction-diffusion models) in one dimension (van Kampen 1992), several variants of which have been used recently in the context of molecular motors (e.g., see Astumian and Bier 1994; Prost et al. 1994; Harms and Lipowsky 1997; Jülicher et al. 1997; Parmeggiani et al. 1999). One important aspect of real motors which should be included in these models is the interdependence of the enzymatic step and the conformational state, as emphasized by the French group (Prost et al. 1994; Jülicher et al. 1997; Parmeggiani et al. 1999). This leads to nonuniform ratchet models in which the transition rates vary with the spatial position of the motor and are localized around certain positions.

Our article is organized as follows. First, we introduce a general class of nonuniform ratchet models in which the molecular motor is described by M internal states and undergoes transitions at K spatial locations within the period of the molecular force potentials. This generalizes previous work on nonuniform ratchets (Prost et al. 1994; Jülicher et al. 1997; Parmeggiani et al. 1999) which was restricted to the case $(M, K) = (2, 2)$. The latter authors used transition rates which are localized with infinite spatial intervals. In contrast, we found it advantageous to parametrize the localized rates in terms of delta functions since this allows us to solve these models analytically. In addition, we will focus on the situation far from chemical equilibrium and detailed balance and, thus, do not address the linear response regime discussed by Parmeggiani et al. (1999).

In the second part of our article, we consider two subclasses of models with $(M, K) = (3, 2)$ and $(M, K) = (2, 2)$ in order to describe the "hand-over-hand" motion of kinesin. As mentioned, these two subclasses correspond to different assumptions about the cooperativity between the two heads of kinesin: the (3, 2)-models describe weakly cooperative heads whereas the (2, 2)-models are for strongly cooperative ones.

Nonuniform ratchet models

The theoretical framework used here is based on the time evolution of the probability densities $P_m(x, t)$ to find the motor at position x and in internal state m which can attain M values $m = 0,\ldots,M-1$. It is tacitly assumed here that displacements of the center-of-mass of the motor which are perpendicular to the filament can be ignored. The position coordinate x measures the displacements of the center-of-mass parallel to the filament.

The different internal states correspond to different internal conformations arising (1) from the chemical reactions between filament, motor, and ATP and (2) from transverse displacements of the center-of-mass of the motor, or (3) from relative displacements of different molecular groups within the motor protein.

In principle, the internal degrees of freedom of the motor could also be described by continuous variables or coordinates, as recently emphasized by Keller and Bustamante (2000). The motor then undergoes stochastic motion within a multi-dimensional state space. We do not pursue such an approach here since the theoretical methods, which are available for the analysis of this multi-dimensional dynamics, are rather limited (Risken 1989; van Kampen 1992).

For a given motor position x and internal state m, the probability density P_m may change (1) because of lateral diffusion in state m described by lateral currents J_m or (2) because of transitions between the different internal states. Therefore, the probability densities P_m satisfy the continuity equations $\partial P_m(x,t)/\partial t + \partial J_m(x,t)/\partial x = I_m(x,t)$ with the transition current densities I_m.

The lateral currents J_m depend on the molecular force potentials $U_m(x)$ and on the external force F which define the effective force potentials:

$$V_m(x) \equiv (U_m(x) - Fx)/T \tag{1}$$

where T is the temperature in energy units. Note that F is the force component which acts tangential to the filament. We use the sign convention that a load force which acts against the motor movement corresponds to $F < 0$. The x-dependence of the molecular interaction potentials $U_m(x)$ is governed by a characteristic length scale denoted by l. For kinesin on microtubules, these potentials are periodic and l represents the potential period with $U_m(x + l) = U_m(x)$.

Using these effective potentials, the lateral currents J_m have the Smoluchowski- or Fokker-Planck form (Risken 1989; van Kampen 1992):

$$J_m(x,t) \equiv -D_0 \left[\frac{\partial}{\partial x} V_m(x) + \frac{\partial}{\partial x}\right] P_m(x,t) \tag{2}$$

where the parameter D_0 represents the small-scale diffusion coefficient. The corresponding friction coefficient ϕ_0 is given by $\phi_0 = T/D_0$, as follows from the Einstein relation.

Note that, in the continuum approach used here, the applied force F, which is conjugate to the parallel coordinate x, must enter linearly into the lateral current as in Eq. (2). In the context of discrete hopping models, a quasi-equilibrium hypothesis leads to transition rates which depend exponentially on the applied force (Fisher and Kolomeisky 1999).

The transition current densities I_m depend on the transition rates $\Omega_{nm} = Omega_{nm}(x)$ from state m to state n and have the generic form:

$$I_m \equiv \sum_n{}' \left[-P_m \Omega_{mn}(x) + P_n \Omega_{nm}(x)\right] \tag{3}$$

where the prime indicates $n \neq m$.

We now want to implement the property of real motors that the biochemical cycle is coupled to the mechanical movement. In the context of ratchets as considered here, this implies that the transitions between

different motor states occur for certain values of x. This has been previously studied for ratchets with $M=2$ internal states and for transitions which are localized at two positions (Prost et al. 1994; Jülicher et al. 1997; Parmeggiani et al. 1999). Here, we generalize this type of model and consider (1) general values of M and (2) transition rates which are localized in space at the discrete set of K positions $x=x_k$ with $k=1,\ldots,K$ and $x_1<x_2<\cdots<x_k$. The latter rates are expressed as:

$$\Omega_{mn}(x) \equiv \sum_k \omega_{mn}(x_k) l_\Omega \delta(x-x_k) \tag{4}$$

where l_Ω represents a molecular length and $\delta(x)$ is Dirac's delta function. As shown below, this parametrization is useful since it allows us to solve these models analytically.

We will now focus on the stationary states with $\partial P_m/\partial t = 0$ and total lateral current $J \equiv \Sigma_m J_m = const.$ It is then convenient to integrate the expressions of Eq. (2), which leads to:

$$e^{Vm(x)} P_m(x) = e^{Vm(x_*)} P_m(x_*) - \frac{1}{D_0} \int_{x_*}^{x} dy e^{Vm(y)} J_m(y) \tag{5}$$

with $V_m(x) = (U_m(x) - Fx)/T$. In addition, we consider the finite interval $0 \le x < l$ and use periodic boundary conditions with the "box normalization":

$$\int_0^l dx\, P(x) = \int_0^l dx \sum_m P_m \equiv 1 \tag{6}$$

which implies one motor per box and, thus, the motor velocity $v=lJ$. For periodic potentials $U_m(x)$, the box size l is equal to the potential period, as mentioned before.

Before we consider explicit examples for the above ratchet models, we will briefly explain how one can obtain the stationary state of these models in general. When the localized transition rates of Eq. (4) are inserted into the densities I_m as in Eq. (3), integration of the continuity equation $\partial J_m/\partial x = I_m$ leads to:

$$J_m(x) = \bar{J}_m + \sum_k \Delta J_m(x_k)\theta(x-x_k) \tag{7}$$

with the average currents $\bar{J}_m$ and the current discontinuities:

$$\Delta J_m(x_k) \equiv \sum_n' [-P_m(x_k) w_{mn}(x_k) + P_n(x_k) w_{nm}(x_k)] l_\Omega \tag{8}$$

Inspection of the last two equations shows that the lateral currents J_m are now expressed in terms of the MK variables $P_m(x_k)$ and the M variables $\bar{J}_m$. Thus, one needs $M(K+1)$ equations in order to determine these $M(K+1)$ unknowns. This set of equations can be obtained as follows.

First, the lateral currents as given by Eq. (7) are inserted into the general relations of Eq. (5) which express the probability densities P_m in terms of the currents J_m. The choice $x_*=x_1$ and $x=x_k$ with $k=2,\ldots,K$ then leads to $M(K-1)$ linear and homogeneous equations for the unknowns $P(x_k)$ and $\bar{J}_m$. In addition, the periodic boundary conditions lead to $2M-1$ linear and homogeneous equations as given by (1) $J_m(x_1+l) = J_m(x_1)$ with $m=0,\ldots,M-2$ and by (2) $P_m(x_1+l) = P_m(x_1)$ with $m=0,\ldots,M-1$. The Mth equation $J_{M-1}(x_1+l) = J_{M-1}(x_1)$ for the currents is not linearly independent since $\Sigma_m \Delta J_m(x_k) = 0$ for all x_k. Finally, the last equation is provided by the normalization condition of Eq. (6), which is a linear but inhomogeneous equation. In this way, one obtains a complete set of $M(K+1)$ linear equations for the $M(K+1)$ unknowns $P(x_k)$ and J_m which can be solved by linear algebra.

Models for dimeric kinesin

The general procedure outlined above will now be applied to the "hand-over-hand" motion of two-headed kinesin. In view of its two heads, both of which can bind to the microtubule, one can distinguish four internal states: (1) A doubly bound state in which both heads are bound to the filament; (2, 3) two excited states, 1 and 2, in which head 1 and head 2 are unbound, respectively; and (4) a completely unbound state in which both heads have been detached.

The excitations from the doubly bound state are induced by the hydrolysis of ATP which may, in general, occur at both heads (Peskin and Oster 1995). If the enzymatic activity of the two heads were completety uncorrelated, the second head could unbind while the other is still in its unbound state. In order to have a motor which is highly processive, such transitions to the completely unbound state must be rare, which requires some sort of cooperative behavior of the two heads. First, we will assume that the heads are weakly cooperative in the sense that the unbound head suppresses the simultaneous unbinding of the other bound head. We may then ignore the completely unbound state and consider three-state models as in Fig. 1.

In the doubly bound state, the center-of-mass of the motor is located at discrete x-positions which are 8 nm apart. The latter states correspond to the minima of the interaction potential $U_0(x)$ which are separated by large potential barriers, as shown schematically in Fig. 1. Now, consider a doubly bound state and let us displace the neck region of the molecular motor using, for example, the tip of an atomic force microscope. In such an experiment, the motor would stay in the doubly bound state for sufficiently small displacements away from the minima, but would detach from the filament if these displacements became too large. Therefore, the potential barriers must be sufficiently large to prevent the motor attaining doubly bound states at intermediate x-values.

If the motor sits in one of these minima, both the trailing and the leading head should be able to adsorb

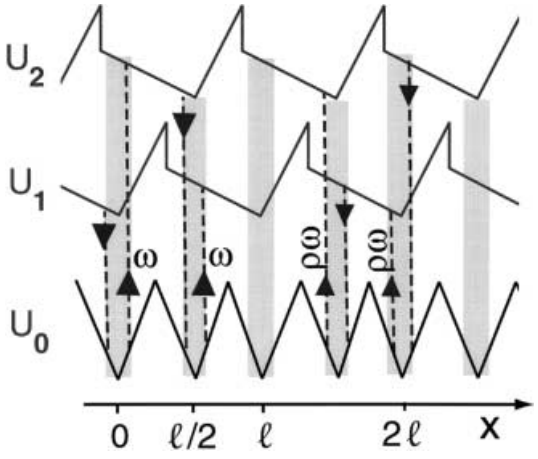

Fig. 1 Molecular interaction potential U_m and transition rates for the three-state model as a function of the motor position x. The doubly bound state corresponds to the potential U_0; the excited states 1 and 2 correspond to unbound heads 1 and 2, respectively. The potential barriers are indicated only in a schematic manner. The transition rates are restricted to the potential minima of U_0. On the *left*, one has a sequence of two excitations of the trailing head with unbinding rate constant ω; on the *right*, a sequence of two excitations of the leading head with unbinding rate constant $\rho\omega$. All transition rates are periodic functions of x with period l, which implies four different rates at each potential minimum of U_0

ATP, unbind from the filament, and then make a forward or a backward step of $l = 16$ nm, respectively. As mentioned, this corresponds to a 8 nm step of the center-of-mass coordinate x. Since both heads are equivalent, the four transition rates from the doubly bound state to the excited states 1 and 2 and back to the doubly bound state must all be periodic with period l (see Fig. 1), and must be related via $\Omega_{02}(x) = \Omega_{01}(x - l/2)$ and $\Omega_{20}(x) = \Omega_{10}(x - l/2)$. Thus, one has to specify only two of the four transition rates, say Ω_{01} and Ω_{10}. The unbinding rate Ω_{01} depends on two rate constants, $\omega_{\rm tr} \equiv \omega$ and $\omega_{\rm le} \equiv \rho\omega$, for the trailing and the leading head, respectively, with $0 \le \rho < 1$, and is given by:

$$\Omega_{01}(x) = \omega l_\Omega \delta(x - l/2) + \rho\omega l_\Omega \delta(x) \tag{9}$$

Likewise, we consider two different rebinding rate constants, $\nu_{\rm tr} \equiv \nu_1$ and $\nu_{\rm le} \equiv \nu_2 > \nu_{\rm tr}$, and the rebinding rate:

$$\Omega_{10}(x) = \nu_1 l_\Omega \delta(x - l/2) + \nu_2 l_\Omega(x) \tag{10}$$

In the two excited states 1 and 2, the motor experiences the microscopic force potentials $U_1(x)$ and $U_2(x)$, respectively, as shown schematically in Fig. 1. Since both heads are equivalent, these two potentials must be related via $U_2(x) = U_1(x - l/2)$.

In principle, the two potentials $U_1(x)$ and $U_2(x)$ represent measurable quantities. Thus, assume that the motor is in the excited state 1 where head 2 is bound and head 1 is unbound. Now, we can imagine to move the unbound head of the motor using again the tip of an atomic force microscope while the other head remains in its bound state. The potential energy of this conformation as a function of the motor position x is described by $U_1(x)$. The bound head 2 represents a strong constraint on the possible locations of the unbound head 1 and, thus, on the position x. It is believed that the unbound head can be displaced by about 16 nm, which corresponds to a displacement of the motor position x by about 8 nm. These displacements are presumably accommodated by the flexibility of the neck region of the dimeric kinesin. Larger separations of the two heads are, however, very unlikely since they would lead to a severe distortion or overstretching of the molecule.

The simplest potential which embodies these features is given by the indented sawtooth potential:

$$\begin{aligned} U_1(x) &= U_{ba} x/l_1 && \text{for } 0 < x < l_1 \\ &= U_{\rm ra}(l - x)/(l - l_1) && \text{for } l_1 < x < l \end{aligned} \tag{11}$$

If the height $U_{\rm ra}$ of the potential ramp is small compared to height $U_{\rm ba}$ of the potential barrier, this indented sawtooth potential has a steep barrier at $x = l_1 < l/2$ as displayed in Fig. 1. Note that the potential ramp corresponds to the range of x-values which are accessible to the motor by displacements of the unbound head, whereas the potential barrier corresponds to those x-values which are inaccessible because of the geometric constraints just discussed.

The stationary state of the three-state ratchet with the transition rates as given by Eqs. (9) and (10) can be determined analytically using the general procedure outlined above. As a result, we find that the motor velocity v has the generic form:

$$v(\omega, F) = v_{\rm res}(F) + [v_{\rm sat}(F) - v_{\rm res}(F)] \frac{\omega}{\omega + \omega_*(F)} \tag{12}$$

for *any* choice of the interaction potentials U_m and of the rebinding rate constants ν_1 and ν_2 (the saturation velocity $v_{\rm sat}$ can vanish for force potentials U_m with certain symmetries which do not lead to directed motion). Thus, the ω-dependence is rather simple whereas the applied force F enters via three functions, the residual velocity $v_{\rm res}$, the saturation velocity $v_{\rm sat}$, and the characteristic rate ω_*.

The residual velocity $v_{\rm res}(F)$ is equal to the velocity in the absence of ATP and, thus, vanishes for zero applied force. Therefore, one obtains the simple hyperbolic relationship:

$$v(\omega, 0) = v_{\rm sat}(0)\omega/(\omega + \omega_*(0)) \quad \text{for } F = 0 \tag{13}$$

which is again *universal* in the sense explained above. This relationship has the same functional form as the well-known Michaelis-Menten relation for enzyme kinetics (Bisswanger 1994). It is important to note, however, that the derivation of the velocity-rate relationship of Eq. (13) did *not* involve any assumptions about the enzyme kinetics of the kinesin heads.

In fact, we will now implement the underlying chemical kinetics and express the unbinding rate constant ω in terms of the ATP concentration Γ. We will divide the biochemical cycle of each head into an unbinding and a rebinding sequence. The unbinding se-

quence contains the adsorption and hydrolysis of ATP and is given by $M/K + ATP \rightarrow M/K/ATP \rightarrow M/K/ADP/P_i \rightarrow M + K/ADP + P_i$, where M, K, and P_i stand for microtubule, kinesin, and inorganic phosphate, respectively. Only the first step of the unbinding sequence depends on the ATP concentration Γ and the associated rate constant is given by $k_1\Gamma$. This implies that the unbinding rate constant ω can be expressed as:

$$\omega^{-1} = (k_1\Gamma)^{-1} + k_2^{-1} \tag{14}$$

which describes Michaelis-Menten kinetics (Bisswanger 1994). The rebinding sequence, on the other hand, consists of $M + K/ADP \rightarrow M/K/ADP \rightarrow M/K + ADP$ and the corresponding rate constants are independent of Γ. If one inserts the expression of Eq. (14) into the velocity-rate relationships as given by Eqs. (12) and (13), one obtains precisely the same functional relationships between the velocity v and Γ but with rescaled (or renormalized) functions v_{sat}, ω_*, and v_{res}.

So far, we have assumed a relatively weak cooperativity between the two heads. Now, let us assume that the heads are strongly cooperative in the sense that the rebinding of the unbound head is strongly correlated with the ATP adsorption of the bound head. Therefore, these two processes can be combined into a single step of the motor cycle, and one may eliminate the intermediate step corresponding to a doubly bound state from the theoretical description. In this way, one arrives at effective two-state models in which the motor undergoes transitions between the two states 1 and 2.

Because of the equivalence of the two heads, the transition rates Ω_{12} and Ω_{21} between the two states are again related and $\Omega_{21}(x) = \Omega_{12}(x - l/2)$. Thus, the two-state model is defined by the unbinding rate:

$$\Omega_{12}(x) = \omega l_\Omega \delta(x) + \rho\omega l_\Omega \delta(x - l/2) \tag{15}$$

with $0 \le \rho < 1$. It turns out that this two-state model again leads to the velocity-rate relationships as given by Eqs. (12) and (13) for all possible molecular interaction potentials.

In general, one may consider models which describe the enzyme kinetics of the two heads in more detail. In the theoretical framework considered here, this leads to ratchet models with an increased number of internal states and with more transitions between these states. In such more detailed models, one may also study different types of synchronization between the two enzymatic cycles of the two heads.

Force dependence of motor properties

Finally, we briefly address the dependence of the motor velocity on the applied force F. We will focus on the simplest case, namely on the two-state model where we choose $\rho = 0$ in Eq. (15) in order to eliminate one parameter from the problem; the more general case with $\rho > 0$ is qualitatively similar. The functional dependence

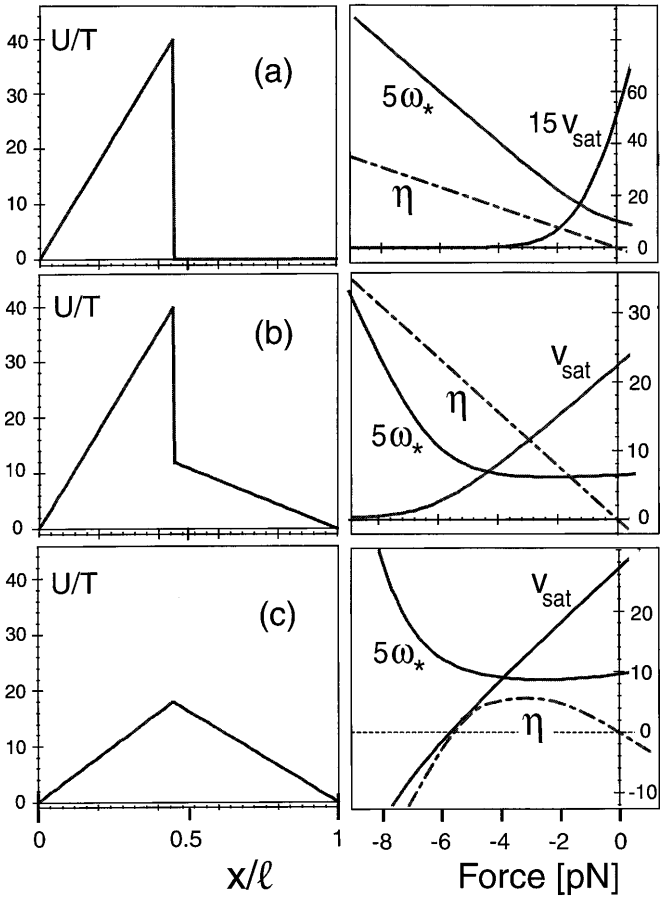

Fig. 2a–c *Left column* Molecular interaction potentials $U \equiv U_1$ in units of temperature T as a function of the coordinate x in units of the potential period l. **a** and **b** are indented sawtooth potentials with steep potential barriers $U_{ba} = 40T$ at $x/l = l_1/l = 9/20$ and with ramp potential $U_{ra} = 0$ and $U_{ra} = 12T$, respectively. **c** A simple sawtooth for comparison with $U_{ba}/T = U_{ra}/T = 18$. *Right column* Force dependence of the saturation velocity v_{sat}, the characteristic rate ω_*, and the efficiency η for the potentials shown on the left. All quantities plotted in the right column are dimensionless; the corresponding units are defined in the text

of v_{sat} and ω_* on the load force $F < 0$ is shown in Fig. 2 for three different choices of the sawtooth potential of Eq. (11). The velocity v_{sat} is plotted in units of the velocity scale $v_{sc} \equiv D_0/l$, the characteristic rate ω_* in units of $\omega_{sc} \equiv 2D_0/ll_\Omega$, and the force F has been transformed into physical units using $F_{sc} \equiv T/l \approx 0.257$ pN.

As mentioned, the molecular interaction potentials should contain a steep barrier reflecting the limited extensibility of the kinesin molecule. In this case, the velocity v_{sat} decreases with increasing load and becomes rather small at a certain characteristic force $F = F_*$. For the examples in Fig. 2a and b, one finds $F_* \approx -2$ pN and -6 pN , respectively. The residual velocity v_{res} is very small in the presence of a steep barrier and can be safely ignored for the force range in Fig. 2. Therefore, the velocity v is proportional to v_{sat}, and $F = F_*$ represents the stall force for the motor.

In Fig. 2c we display, for comparison, the behavior for a simple sawtooth potential without a steep barrier,

as used previously in the context of two-state models (Prost et al. 1994; Jülicher et al. 1997). In this case, the velocity v_{sat} goes through zero at $F = F_*$ and becomes negative for $F < F_*$. Furthermore, the residual velocity v_{res} can no longer be ignored since forces of the order of F_* will frequently push the motor over the relatively small potential barriers.

Another important quantity which characterizes the performance of the motor is its efficiency η, which can be easily determined in our models. First, one has to calculate the unbinding current J_{unb} for the stationary state, which is equal to the number of unbinding transitions per unit time and per motor. In the two-state model with $\rho = 0$ as discussed here, the unbinding current is given by

$$J_{unb} = [P_1(0) + P_2(l/2)]\omega l_\Omega \qquad (16)$$

The efficiency η is then given by $\eta = |F|v/\Delta G J_{unb}$, where ΔG is the free energy consumed per unbinding transition. Using the dimensionless force $\bar{F} \equiv F/F_{sc} = lF/T$, the dimensionless velocity $\bar{v} \equiv v/v_{sc} = lv/D_0$, and the dimensionless unbinding current $\bar{J}_{unb} \equiv J_{unb}/J_{sc} = l^2 J_{unb}/2D_0$ one obtains $\eta = (T/2\Delta G)\bar{F}\bar{v}/\bar{J}_{unb}$ which defines the natural efficiency scale $\eta_{sc} \equiv T/2\Delta G$.

In Fig. 2 the efficiency η is plotted in units of η_{sc}. In general, η depends on ω. For the indented sawtooth potentials in Fig. 2a and b, this dependence is negligible over the displayed range of forces. For the simple sawtooth in Fig. 2c, on the other hand, the plotted efficiency corresponds to the limit of large ω. As ω is decreased, the velocity v decreases and the left part of the η-curve is shifted towards the right.

It is interesting to note that, for the indented sawtooth potentials, the efficiency η increases monotonically for increasing load up to and beyond the stall force, whereas it goes through zero for the simple sawtooth potential. If the motor consumes one ATP per unbinding transition, one has $\eta_{sc} = 1/40$, which implies that the efficiency for $F = -5$ pN is about 49% for the indented sawtooth in Fig. 2b and only about 8% for the simple sawtooth in Fig. 2c. Note that the behavior for the indented sawtooth potential with $\rho = 0$ corresponds to "tight coupling" between the enzymatic cycle and the mechanical movement. In the models considered here, "loose coupling" can arise from $\rho > 0$ corresponding to active backwards steps or from reduced potential barriers which allow diffusive steps in the backwards direction.

Conclusion

In summary, we have introduced a general class of nonuniform ratchet (or reaction-diffusion) models with M internal states and transitions at K spatial locations. We have determined the functional dependence of the motor velocity v on the unbinding rate constant ω (and, thus, on the ATP concentration Γ) for two subclasses of models with $(M, K) = (3, 2)$ and $(M, K) = (2, 2)$, which correspond to weakly and strongly cooperative heads, respectively. In both cases, we found the same universal relationships between v and ω as given by Eqs. (12) and (13).

It is possible to determine the velocity-concentration relationship for all nonuniform ratchet models with arbitrary values of M and K (R. Lipowsky, unpublished results). One then finds that the relationship of Eq. (12) is always valid if the motor cycle contains only *one* ATP-dependent transition rate per motor cycle. It should be noted, however, that the three-state and the two-state models considered here contain *four* or *two* ATP-dependent transition rates per motor cycle. In general, the velocity-concentration relationship depends on the number of ATP-dependent transition rates (R. Lipowsky, unpublished results). Thus, (M, K) models with two and four ATP-dependent transition rates are characterized by velocity-concentration relationships which can be somewhat more complex than the form given by Eq. (12). However, these more general relationships reduce to Eq. (12) if the (M, K) models contain certain symmetries or constraints. Such a reduction applies to the two subclasses of models with $(M, K) = (3, 2)$ and $(M, K) = (2, 2)$ as studied here for two-headed kinesin.

Acknowledgement We thank Michael E. Fisher for useful comments on this manuscript.

References

Astumian R, Bier M (1994) Fluctuation driven ratchets: molecular motors. Phys Rev Lett 72: 1766–1769
Bisswanger H (1994) Enzymkinetik. VCH, Weinheim
Fisher ME, Kolomeisky A (1999) The force exerted by a molecular motor. Proc Natl Acad Sci USA 96: 6597–6602
Gilbert S, Moyer M, Johnson K (1998) Alternating site mechanism of the kinesin ATPase. Biochemistry 37: 792–799
Hancock WO, Howard J (1998) Processivity of the motor protein kinesin requires two heads. J Cell Biol 140: 1395–1405
Harms T, Lipowsky R (1997) Driven ratchets with frozen disorder. Phys Rev Lett 79: 2895–2898
Howard J, Hudspeth AJ, Vale RD (1989) Movement of microtubules by single kinesin molecules. Nature 342: 154–158
Hua W, Young EC, Fleming ML, Gelles J (1997) Coupling of kinesin steps to ATP hydrolysis. Nature 388: 390–393
Jülicher F, Ajdari A, Prost J (1997) Modeling molecular motors. Rev Mod Phys 69: 1269–1281
Kampen N van (1992) Stochastic processes in physics and chemistry. Elsevier, Amsterdam
Keller D, Bustamante C (2000) The mechanochemistry of molecular motors. Biophys J 78: 541–556
Parmeggiani A, Jülicher F, Ajdari A, Prost J (1999) Energy transduction of isothermal ratchets: generic aspects and specific examples close to and far from equilibium. Phys Rev E 60: 2127–2140
Peskin C, Oster G (1995) Coordinated hydrolysis explains the mechanical behavior of kinesin. Biophys J 68: 202s–210s
Prost J, Chauwin J-F, Peliti L, Ajdari A (1994) Asymmetric pumping of particles. Phys Rev Lett 72: 2652–2655
Risken H (1989) The Fokker-Planck equation: methods of solution and applications. Springer, Berlin Heidelberg New York
Schnitzer MJ, Block SM (1997) Kinesin hydrolyses one ATP per 8 nm step. Nature 388: 386–390

Svoboda K, Schmidt C, Schnapp B, Block S (1993) Direct observation of kinesin stepping by optical trapping interferometry. Nature 365: 721–727

Thormählen M, Marx A, Müller S-A, Song Y-H, Mandelkow E-M, Aebi U, Mandelkow E (1998) Interaction of monomeric and dimeric kinesin with microtubules. J Mol Biol 275: 795–809

Visscher K, Schnitzer MJ, Block SM (1999) Single kinesin molecules studied with a molecular force clamp. Nature 400: 184–189